

# VII. QCD, jets and gluons

- ❖ *Quantum Chromodynamics (QCD)*: the theory of strong interactions
  - ☉ Interactions are carried out by a massless spin-1 particle – *gauge boson*
  - ☉ In quantum electrodynamics (QED) gauge bosons are photons, in QCD – *gluons*
  - ☉ Gauge bosons couple to conserved charges: photons in QED – to electric charges, and gluons in QCD – to colour charges
- ❖ Gluons have electric charge of 0 and couple only to colour charges  $\Rightarrow$  strong interactions are **flavour-independent**

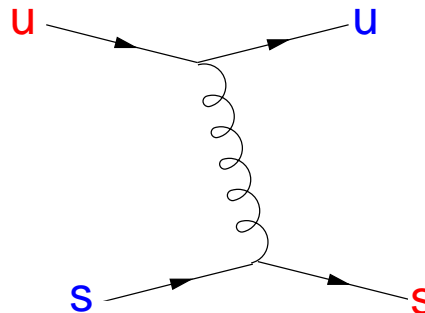


Figure 65: Gluon exchange between quarks

## ❖ Gluons carry colour charges themselves!

Colour quantum numbers are conserved  $\Rightarrow$  for the gluon on Figure 65:

$$I_3^C = I_3^C(r) - I_3^C(b) = 1/2 - 0 = 1/2 \quad (102)$$

$$Y^C = Y^C(r) - Y^C(b) = 1/3 - (-2/3) = 1 \quad (103)$$

In general, gluons exist in 8 different colour states:

Gluon colour wavefunction $\chi_{gi}^C$	$I_3^C$	$Y^C$
$\bar{r}g$	1	0
$\bar{g}r$	-1	0
$\bar{r}b$	1/2	1
$\bar{g}b$	-1/2	-1
$\bar{g}b$	-1/2	1
$\bar{r}b$	1/2	-1
$(\bar{g}\bar{g}-\bar{r}\bar{r})/\sqrt{2}$	0	0
$(\bar{g}\bar{g}-\bar{r}\bar{r}-2\bar{b}\bar{b})/\sqrt{6}$	0	0

## ❖ Gluons hence can couple to other gluons!

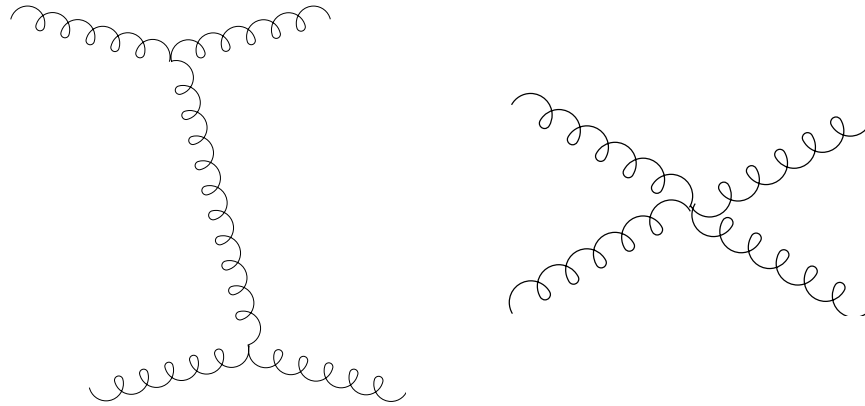


Figure 66: Lowest-order contributions to gluon-gluon scattering

- ◎ Bound colourless states of gluons are called *glueballs* (not detected experimentally yet)
- ◎ Gluons are massless  $\Rightarrow$  long-range interaction (still, not free particles unlike  $\gamma$ )
- ❖ Principle of *asymptotic freedom* (1973 - Gross, Politzer, Wilczek):
  - ◎ At short distances between particles, strong interactions are sufficiently weak (lowest order diagrams)  $\Rightarrow$  quarks and gluons are essentially free particles
  - ◎ At large distances, high-order diagrams dominate  $\Rightarrow$  many coloured objects, “anti-screening” of colour charge  $\Rightarrow$  interaction is very strong

Asymptotic freedom thus implies the requirement of colour confinement

- ⊙ Due to the complexity of high-order diagrams, the very process of confinement can not be calculated analytically  $\Rightarrow$  only numerical models are available

### **Strong coupling constant $\alpha_s$**

At short distances, quark-antiquark potential is:

$$V(r) = -\frac{4}{3} \frac{\alpha_s}{r} \quad (r < 0.1 \text{ fm}) \quad (104)$$

- ⊙ Constant  $\alpha_s$  is QCD analogue of  $\alpha_{em}$  and is a measure of the interaction strength

However,  $\alpha_s$  is a “*running constant*”, and increases with increase of  $r$ , becoming divergent at very big distances.

- ❖ At large distances, quarks are subject to the “*confining potential*” which grows with  $r$ :

$$V(r) \approx \lambda r \quad (r > 1 \text{ fm}) \quad (105)$$

❖ **Short** distance interactions are associated with the **large** momentum transfer  $\bar{q}$  between the particles:

$$|\vec{q}| = O(r^{-1}) \quad (106)$$

☉  $\alpha_s$  is decreasing with increasing momentum transfer

In general, if interaction involves energy exchange, too, Lorentz-invariant energy-momentum transfer  $Q$  is defined as

$$Q^2 = \vec{q}^2 - E_q^2 \quad (107)$$

In the *leading order* of QCD,  $\alpha_s$  dependency on  $Q$  is given by

$$\alpha_s = \frac{12\pi}{(33 - 2N_f) \ln(Q^2 / \Lambda^2)} \quad (108)$$

Here  $N_f$  is the number of allowed quark flavours, and  $\Lambda \approx 0.2$  GeV is the QCD scale parameter which has to be defined experimentally.

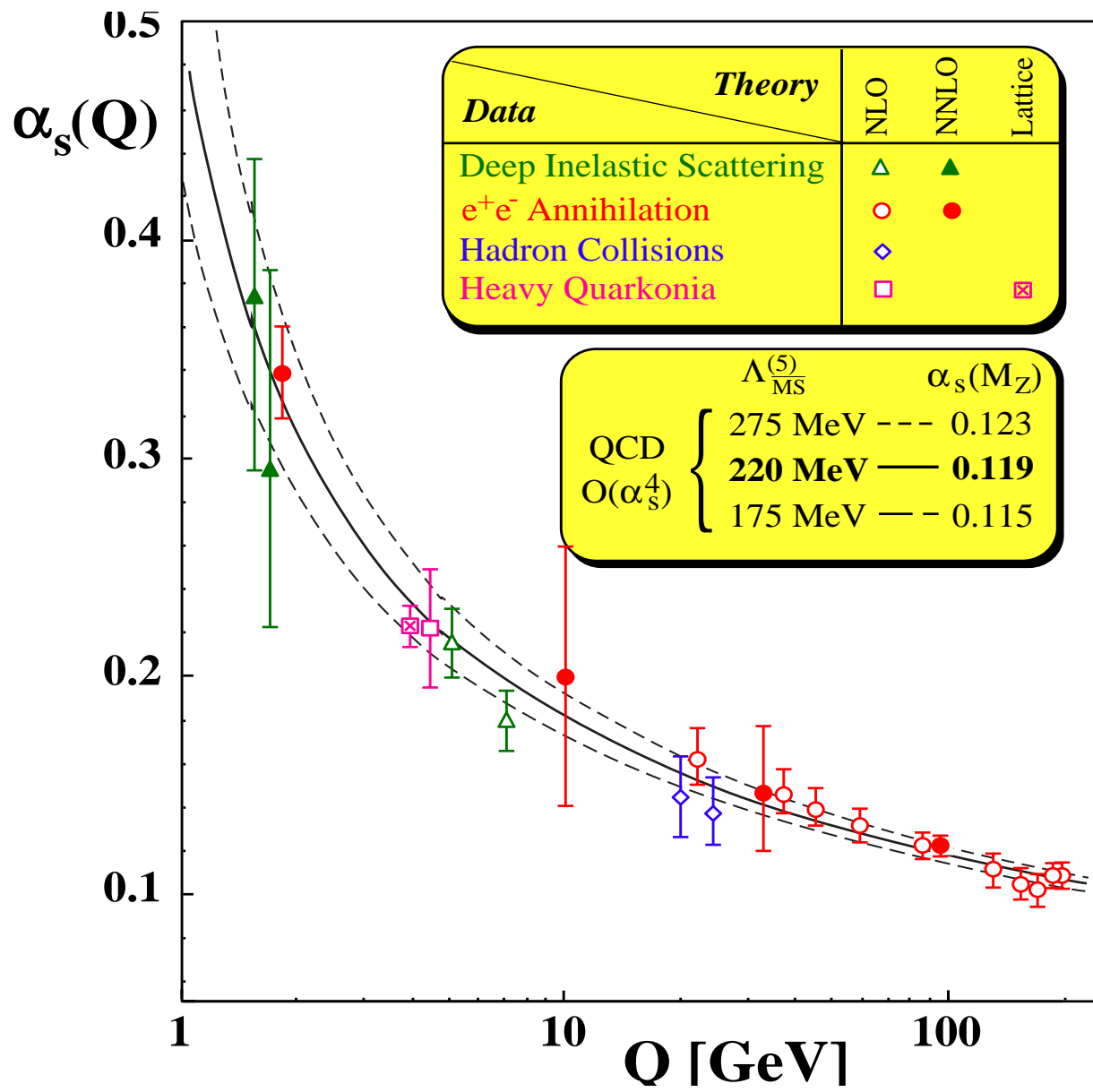


Figure 67: Running of  $\alpha_s$ , experimental data vs theory

# Electron-positron annihilation

❖ A perfect laboratory for precision studies of QCD:

$$e^+ + e^- \rightarrow \gamma^* \rightarrow \text{hadrons} \quad (109)$$

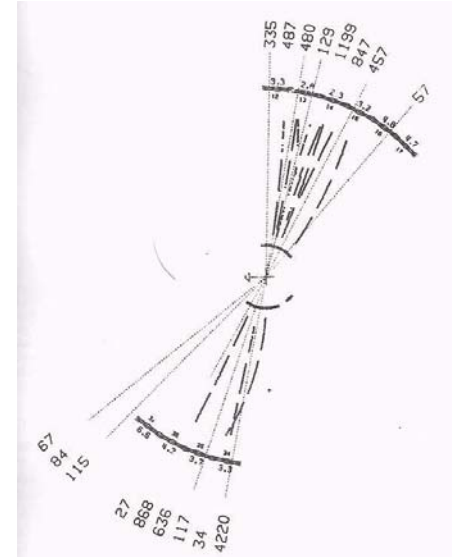
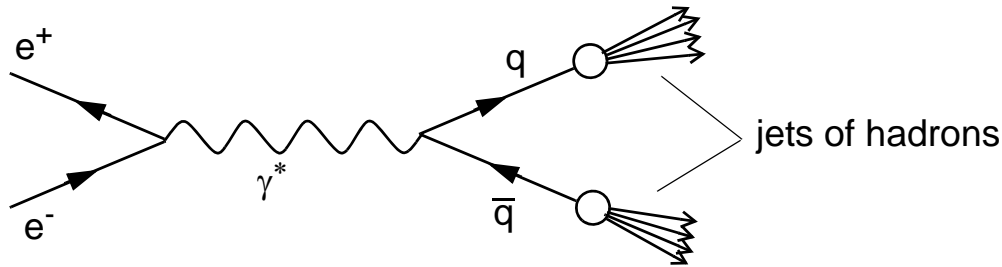


Figure 68:  $e^+e^-$  annihilation into hadrons (JADE experiment display, 1979)

- ☉ At energies between  $\sim 12$  GeV and  $\sim 45$  GeV per beam,  $e^+e^-$  annihilation produces a photon which converts into a quark-antiquark pair
- ☉ Quark and antiquark *fragment* into observable hadrons

- ⊙ When beam energies are equal, quark and antiquark momenta are equal and counterparallel  $\Rightarrow$  hadrons are produced in two opposing *jets* of equal energies
- ⊙ Direction of a jet reflects direction of a corresponding quark

Compare the process (109) with the reaction

$$e^+ + e^- \rightarrow \gamma^* \rightarrow \mu^+ + \mu^- \quad (110)$$

Angular distribution of muons (spin 1/2) can be calculated as:

$$\frac{d\sigma}{d\cos\theta}(e^+e^- \rightarrow \mu^+\mu^-) = \frac{\pi\alpha^2}{2Q^2}(1 + \cos^2\theta) \quad (111)$$

where  $\theta$  is the production angle with respect to the initial electron direction in center-of-mass frame.

- ❖ If quarks, like muons, have spin 1/2, angular distribution of jets goes like  $(1+\cos^2\theta)$ ; if quarks have spin 0 – like  $(1-\cos^2\theta)$



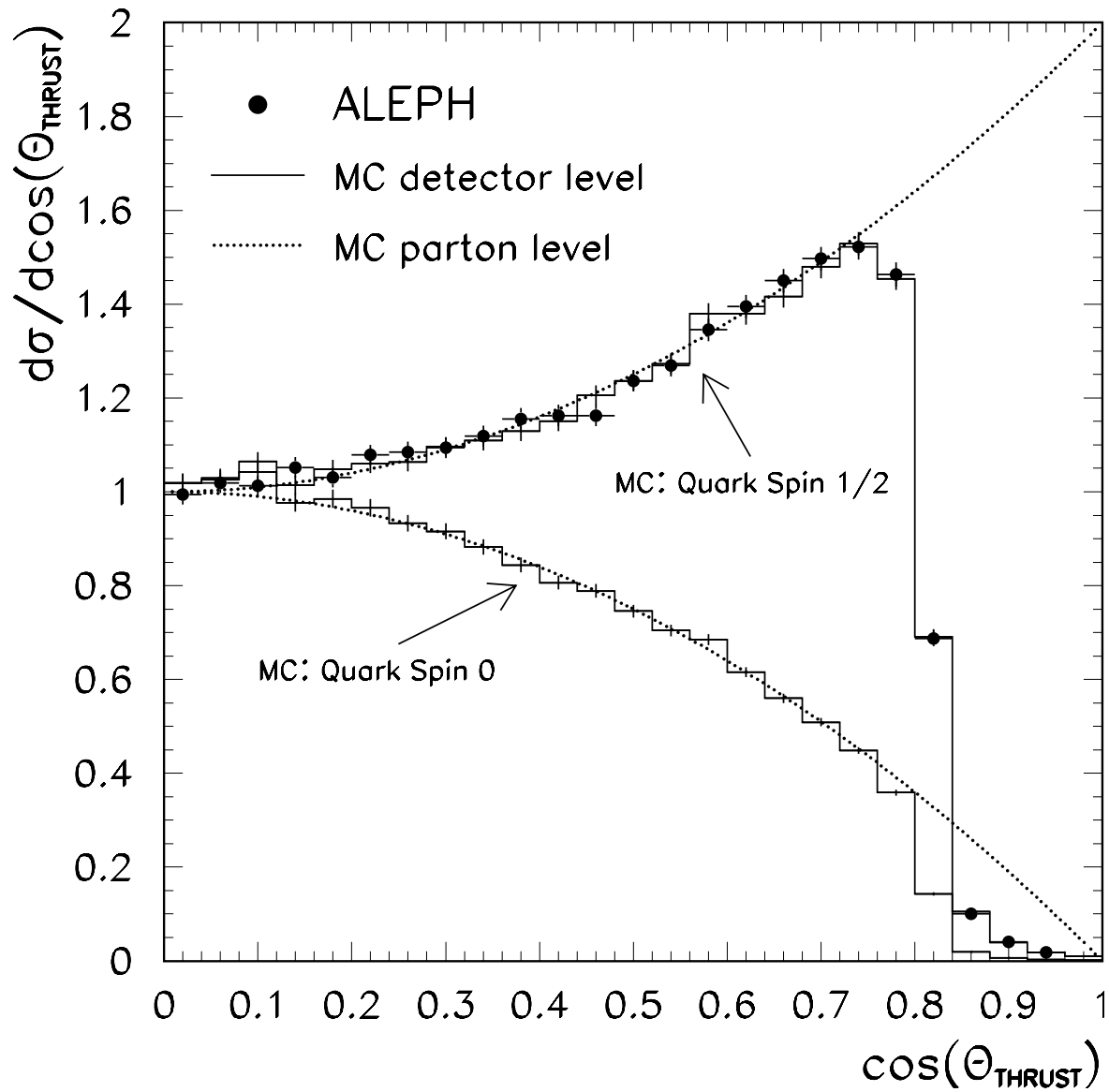



Figure 69: Angular distribution of the quark jet in  $e^+e^-$  annihilation, compared with models (ALEPH experiment at LEP, 1992-1994)

For a quark-antiquark pair,

$$\frac{d\sigma}{d\cos\theta}(e^+e^- \rightarrow q\bar{q}) = 3e_q^2 \frac{d\sigma}{d\cos\theta}(e^+e^- \rightarrow \mu^+\mu^-) \quad (112)$$

where the fractional charge of a quark  $e_q$  is taken into account and factor 3 arises from number of colours.

- ❖ Experimentally measured angular dependence is clearly proportional to  $(1+\cos^2\theta) \Rightarrow$  jets are aligned with spin-1/2 particles – quarks
- ❖ If a high-momentum (hard) gluon is emitted by a quark or antiquark, it fragments to a jet of its own, which leads to a three-jet event
  - 🎯 Observation of three-jet events in  $e^+e^-$  annihilation at PETRA accelerator (DESY, Hamburg) in 1979 is credited as gluon discovery

	DELPHI	Run: 53578	Evt: 12239
	Beam: 45.6 GeV	Proc: 25-Sep-1996	
	DAS: 14-Oct-1994	Scan: 30-Sep-1996	
		21:07:03	Tan+DST

	TD	TE	TS	TK	TV	ST	PA
Act	0	190	0	31	0	0	0
	( 0 )	( 289 )	( 0 )	( 31 )	( 0 )	( 0 )	( 0 )
Deact	0	0	0	0	0	0	0
	( 0 )	( 0 )	( 0 )	( 6 )	( 0 )	( 0 )	( 0 )

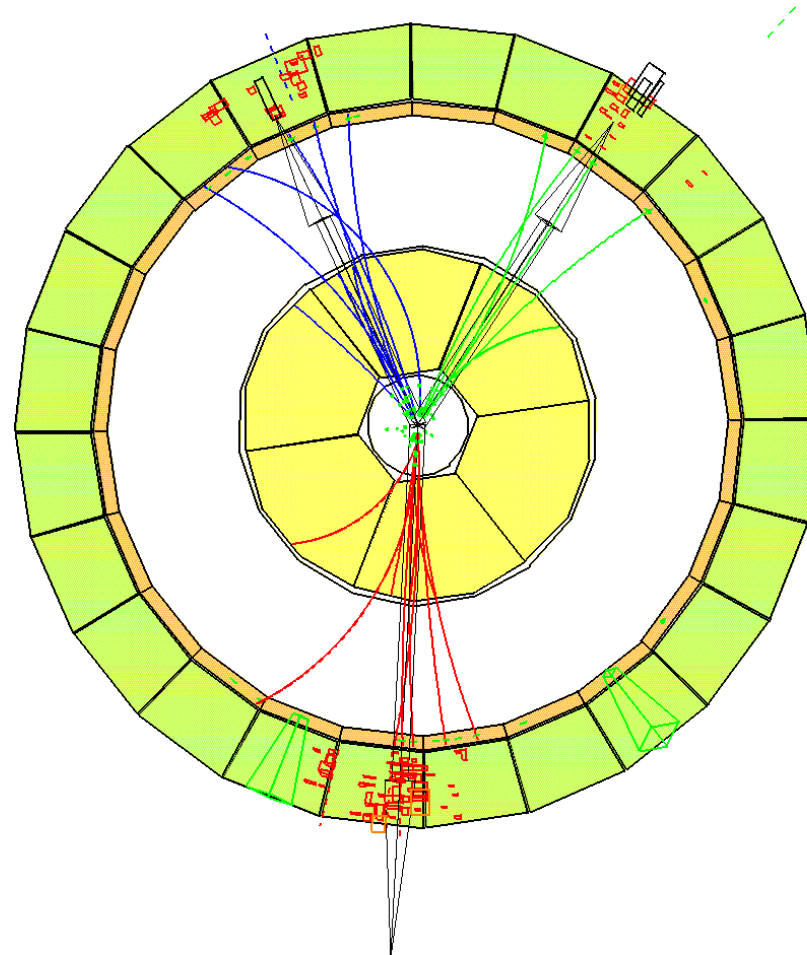


Figure 70: A three-jet event in  $e^+e^-$  annihilation as seen by the DELPHI experiment at LEP (1996)

- ❖ In three-jet events, it is difficult to distinguish which of the jets belongs to the gluon, hence a specific sensitive variable has to be chosen

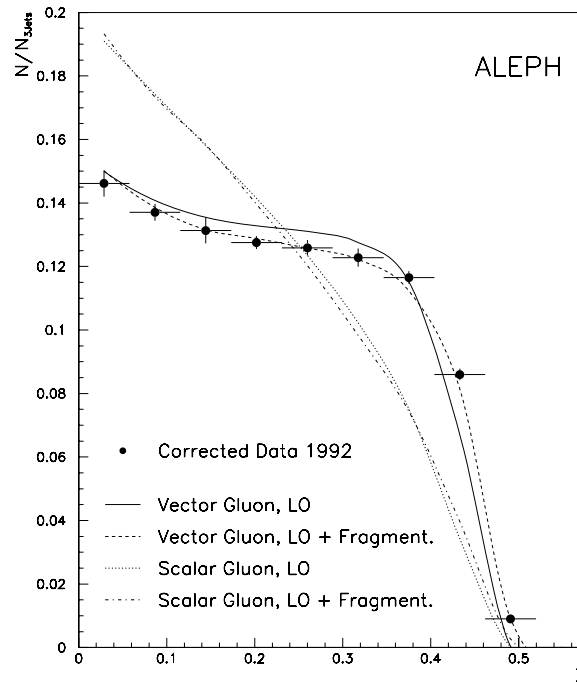


Figure 71: Distribution of  $Z$  (as in Eq.(113)) in 3-jet  $e^+e^-$  annihilation events, compared with models

- 🎯 Jets are ranked by energies  $E_1 > E_2 > E_3$  ( $E_1$  ought to be a quark), and  $Z$  is:

$$Z = \frac{1}{\sqrt{3}}(E_2 - E_3) \tag{113}$$

- ❖ Angular distributions of jets confirm models where quarks are spin-1/2 fermions and gluons are spin-1 bosons
- ❖ Observed rate of three-jet to two-jet events can be used to determine value of  $\alpha_s$  (probability for a quark to emit a gluon is determined by  $\alpha_s$ ):

$$\alpha_s = 0.15 \pm 0.03 \quad \text{for } E_{\text{CM}} = 30 \text{ to } 40 \text{ GeV}$$

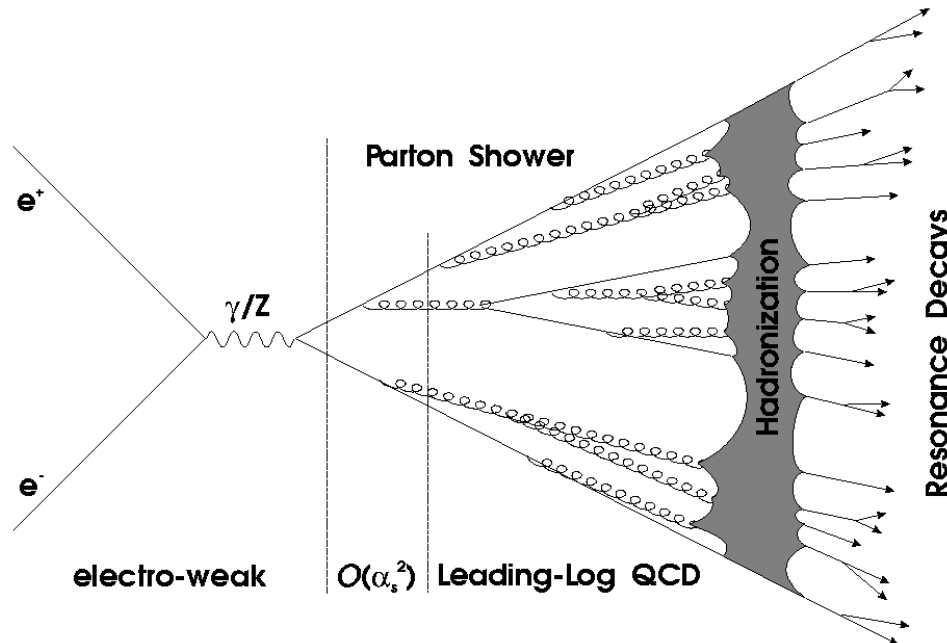


Figure 72: Principal scheme of hadroproduction in  $e^+e^-$  annihilation. Hadronization (=fragmentation) begins at distances of order 1 fm between partons

The *total cross-section* of  $e^+e^- \rightarrow hadrons$  is often expressed as in Eq.(81):

$$R \equiv \frac{\sigma(e^+e^- \rightarrow hadrons)}{\sigma(e^+e^- \rightarrow \mu^+\mu^-)} \quad (114)$$

where the denominator is (see also Eq.(82))

$$\sigma(e^+e^- \rightarrow \mu^+\mu^-) = \frac{4\pi\alpha^2}{3Q^2} \quad (115)$$

Using the same argumentation as in Eq.(112) and assuming that the main contribution comes from quark-antiquark two-jet events,

$$\sigma(e^+e^- \rightarrow hadrons) = \sum_q \sigma(e^+e^- \rightarrow q\bar{q}) = 3 \sum_q e_q^2 \sigma(e^+e^- \rightarrow \mu^+\mu^-) \quad (116)$$

and hence

$$R = 3 \sum_q e_q^2$$

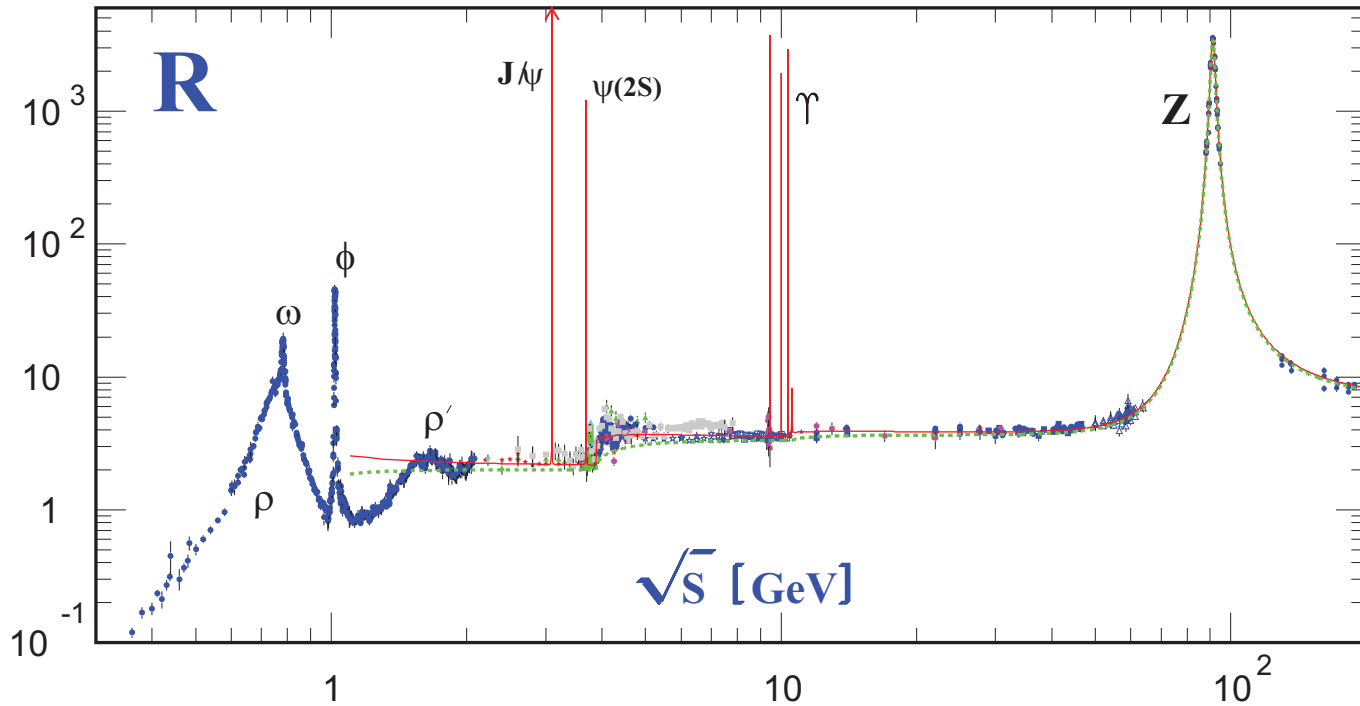


Figure 73: Measured  $R$  (Eq.(114)) with theoretical predictions for five available flavours (u,d,s,c,b), using two different  $\alpha_s$  calculations

❖  $R$  is a good probe for both number of colours in QCD and number of quark flavours allowed to be produced at a given  $Q$ : from Eq.(116) it follows that:

$$R(u,d,s)=2 ; R(u,d,s,c)=10/3 ; R(u,d,s,c,b)=11/3$$

If the radiation of hard gluons is taken into account, the extra factor proportional to  $\alpha_s$  arises:

$$R = 3 \sum_q e_q^2 \left( 1 + \frac{\alpha_s(Q^2)}{\pi} \right) \tag{117}$$

**Elastic electron scattering**

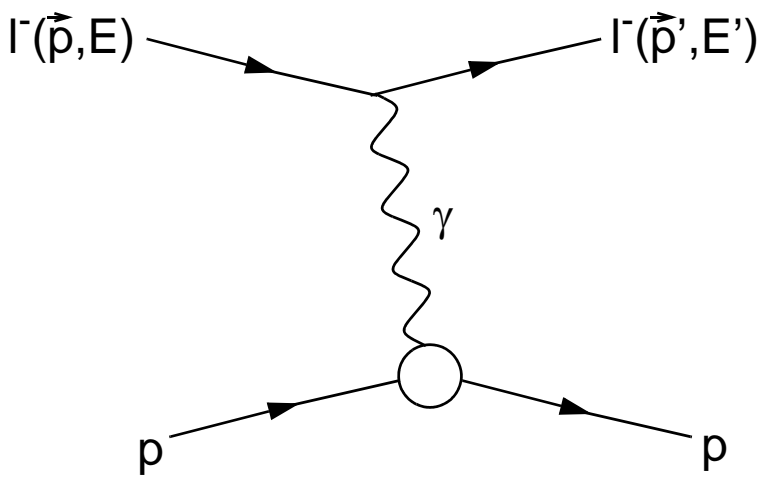


Figure 74: Dominant one- $\gamma$  exchange process for elastic lepton-proton scattering

❖ Elastic scattering: particles nature does not change



- ❖ Beams of structureless leptons (electron, positron) are a good “probe” for investigating properties of hadrons
- ❖ Elastic lepton-hadron scattering have been used to measure sizes of hadrons

Angular distribution of an electron of momentum  $p \ll m$  scattered by a static electric charge  $e$  is described by the Rutherford formula:

$$\left(\frac{d\sigma}{d\Omega}\right)_R = \frac{m^2 \alpha^2}{4p^2 \sin^4(\theta/2)} \quad (118)$$

Here  $\Omega$  is the solid angle of a scattered particle,  $\theta$  is its azimuthal angle

If the electric charge is not point-like, but is spread with a spherically symmetric density distribution, i.e.,  $e \rightarrow e\rho(r)$ , where  $\rho(r)$  is normalized:

$$\int \rho(r) d^3\vec{x} = 1$$

then the differential cross-section (118) is replaced by

$$\frac{d\sigma}{d\Omega} = \left( \frac{d\sigma}{d\Omega} \right)_R G_E^2(q^2) \quad (119)$$

where the *electric form factor*

$$G_E(q^2) = \int \rho(r) e^{i\vec{q} \cdot \vec{x}} d^3\vec{x} \quad (120)$$

is the Fourier-transform of  $\rho(r)$  with respect to the momentum transfer  $\vec{q} = \vec{p} - \vec{p}'$ .

– For  $q = 0$ ,  $G_E(0) = 1$  (low momentum transfer)

– For  $q^2 \rightarrow \infty$ ,  $G_E(q^2) \rightarrow 0$  (large momentum transfer)

❖ Measurements of the cross-section (119) determine the form-factor and hence the charge distribution inside the proton

For example, the RMS charge radius is given by

$$r_E^2 \equiv \overline{r^2} = \int r^2 \rho(r) d^3\vec{x} = -6 \left. \frac{dG_E(q^2)}{dq^2} \right|_{q^2=0} \quad (121)$$

- ❖ In addition to  $G_E$ , there is also  $G_M$  – the *magnetic form factor*, associated with the magnetic moment distribution within the proton
- ❖ At high momentum transfers, the *recoil energy* of the proton is not negligible, and  $\vec{q}$  is replaced by the Lorentz-invariant  $Q$ , given by

$$Q^2 = (\vec{p} - \vec{p}')^2 - (E - E')^2 \quad (122)$$

- ☉ at high  $Q$ , static interpretation of charge and magnetic moment distribution breaks down
- ☉ Eq.(121) is valid only for low  $Q^2 = q^2$ .

For a high-energy electron ( $m \ll E$ ), and taking into account magnetic moment of the electron itself, one obtains:

$$\frac{d\sigma}{d\Omega} = \frac{\alpha^2}{4E^2 \sin^4(\theta/2)} \left(\frac{E'}{E}\right) \left[ G_1(Q^2) \cos^2\left(\frac{\theta}{2}\right) + 2\tau G_2(Q^2) \sin^2\left(\frac{\theta}{2}\right) \right] \quad (123)$$

Here  $E'$  is electron's energy after scattering, and

$$G_1(Q^2) = \frac{G_E^2 + \tau G_M^2}{1 + \tau}; \quad G_2(Q^2) = G_M^2; \quad \tau = \frac{Q^2}{4M_p^2}$$

and form factors are normalized so that

$$G_E(0) = 1 \text{ and } G_M(0) = \mu_p = 2.79$$

❖ Experimentally, it is sufficient to measure  $E'$  and  $\theta$  of outgoing electrons in order to derive  $G_E$  and  $G_M$  using Eq.(123)

Results of proton size measurements are conveniently divided into three  $Q^2$  regions: low, intermediate and high

- ❖ low  $Q^2 \Rightarrow \tau$  is very small  $\Rightarrow G_E$  dominates the cross-section and  $r_E$  can be precisely measured:

$$r_E = 0.85 \pm 0.02 \text{ fm} \quad (124)$$

- ❖ intermediate range:  $0.02 \leq Q^2 \leq 3 \text{ GeV}^2 \Rightarrow$  both  $G_E$  and  $G_M$  give sizeable contribution  $\Rightarrow$  they can be defined e.g. through a parameterization:

$$G_E(Q^2) \approx \frac{G_M(Q^2)}{\mu_p} \approx \left( \frac{\beta^2}{\beta^2 + Q^2} \right)^2 \quad (125)$$

with  $\beta^2 = 0.84 \text{ GeV}^2$

- ❖ high  $Q^2 > 3 \text{ GeV}^2 \Rightarrow$  only  $G_M$  can be measured accurately

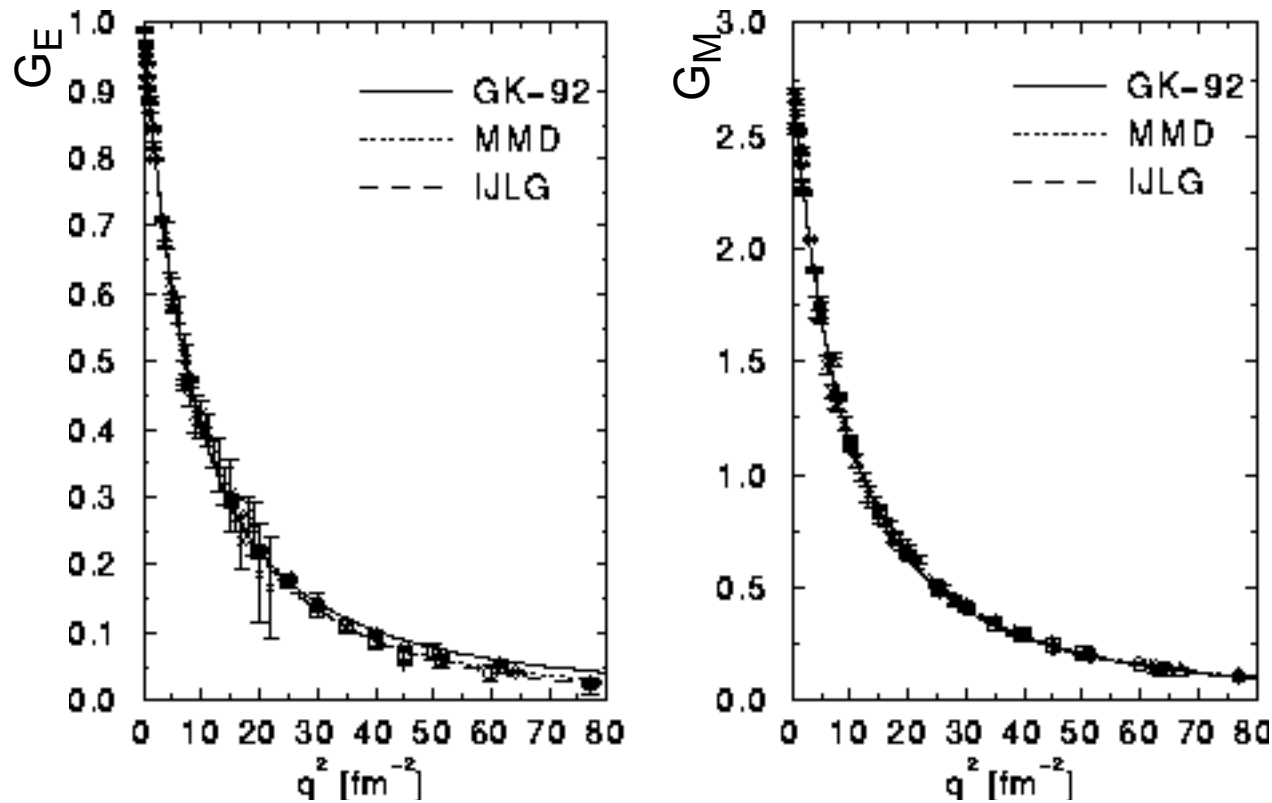


Figure 75: Electric and magnetic proton form-factors, compared with different parameterizations

- ❖ Such form-factor behaviour (e.g.,  $G_E \neq 1$ ) indicates that proton is **not** a point-like structure

# Inelastic lepton scattering

- ❖ Historically, was first to give evidence of quarks in protons
- 🎯 In what follows, only one-photon exchange is considered

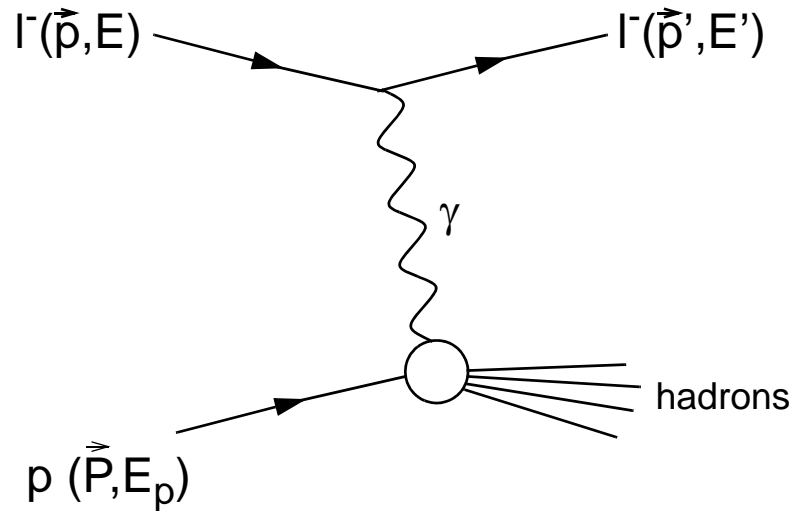


Figure 76: One-photon exchange in inelastic lepton-proton scattering

- ❖ The exchanged photon acts as a probe of the proton structure
- ❖ Momentum transfer  $\vec{p} - \vec{p}'$  must be **big** enough to cause very **small** photon wavelength, small enough to probe a proton

- ❖ When a photon resolves a quark within a proton, the total lepton-proton scattering is a two-step process:

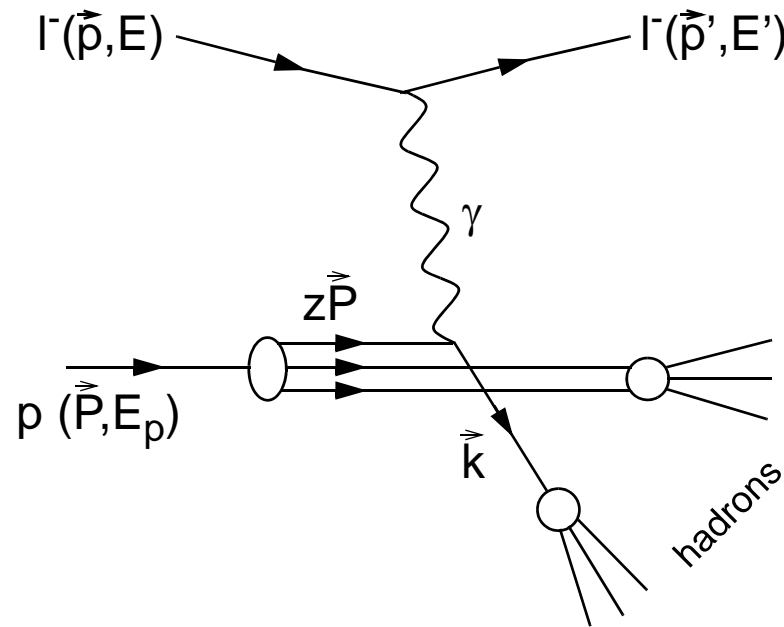


Figure 77: Detailed picture of deep-inelastic lepton-proton scattering

- 1) First step: elastic scattering of the lepton from one of the quarks:

$$l^- + q \rightarrow l^- + q \quad (l = e, \mu)$$

- 2) Second step: fragmentation of the *recoil quark* and the proton remnant into observable hadrons



- ❖ Angular distributions of recoil leptons reflect properties of quarks from which they scattered

For further studies, some new variables have to be defined:

- ❖ Lorentz-invariant generalization for the transferred energy  $\nu$ :

$$2M_p \nu \equiv W^2 + Q^2 - M_p^2 \quad (126)$$

where  $W$  is the invariant mass of the final hadron state; in the rest frame of the proton  $\nu = E - E'$

- ❖ Dimensionless scaling variable  $x$ :

$$x \equiv \frac{Q^2}{2M_p \nu} \quad (127)$$

For  $Q \gg M_p$  and a very large proton momentum  $\vec{P} \gg M_p$ ,  $x$  is the *fraction* of the proton momentum carried by the struck quark;  $0 \leq x \leq 1$

- ❖ Energy  $E'$  and angle  $\theta$  of scattered lepton are independent variables, describing inelastic process

$$\frac{d\sigma}{dE' d\Omega'} = \frac{\alpha^2}{4E^2 \sin^4\left(\frac{\theta}{2}\right)} \frac{1}{v} \left[ \cos^2\left(\frac{\theta}{2}\right) F_2(x, Q^2) + \sin^2\left(\frac{\theta}{2}\right) \frac{Q^2}{xM_p^2} F_1(x, Q^2) \right] \quad (128)$$

⊙ Form (128) is a generalization of the elastic scattering formula (123)

⊙ *Structure functions*  $F_1$  and  $F_2$  parameterize the interaction at the quark-photon vertex (just like  $G_1$  and  $G_2$  parameterized the elastic scattering)

- ❖ *Bjorken scaling* (a.k.a *scale invariance*) was observed by many experiments:

$$F_{1,2}(x, Q^2) \approx F_{1,2}(x) \quad (129)$$

At  $Q \gg M_p$ , structure functions are approximately independent on  $Q^2$ .

⊙ Meaning: if all particle masses, energies and momenta are multiplied by a scale factor, structure functions at any given  $x$  remain unchanged

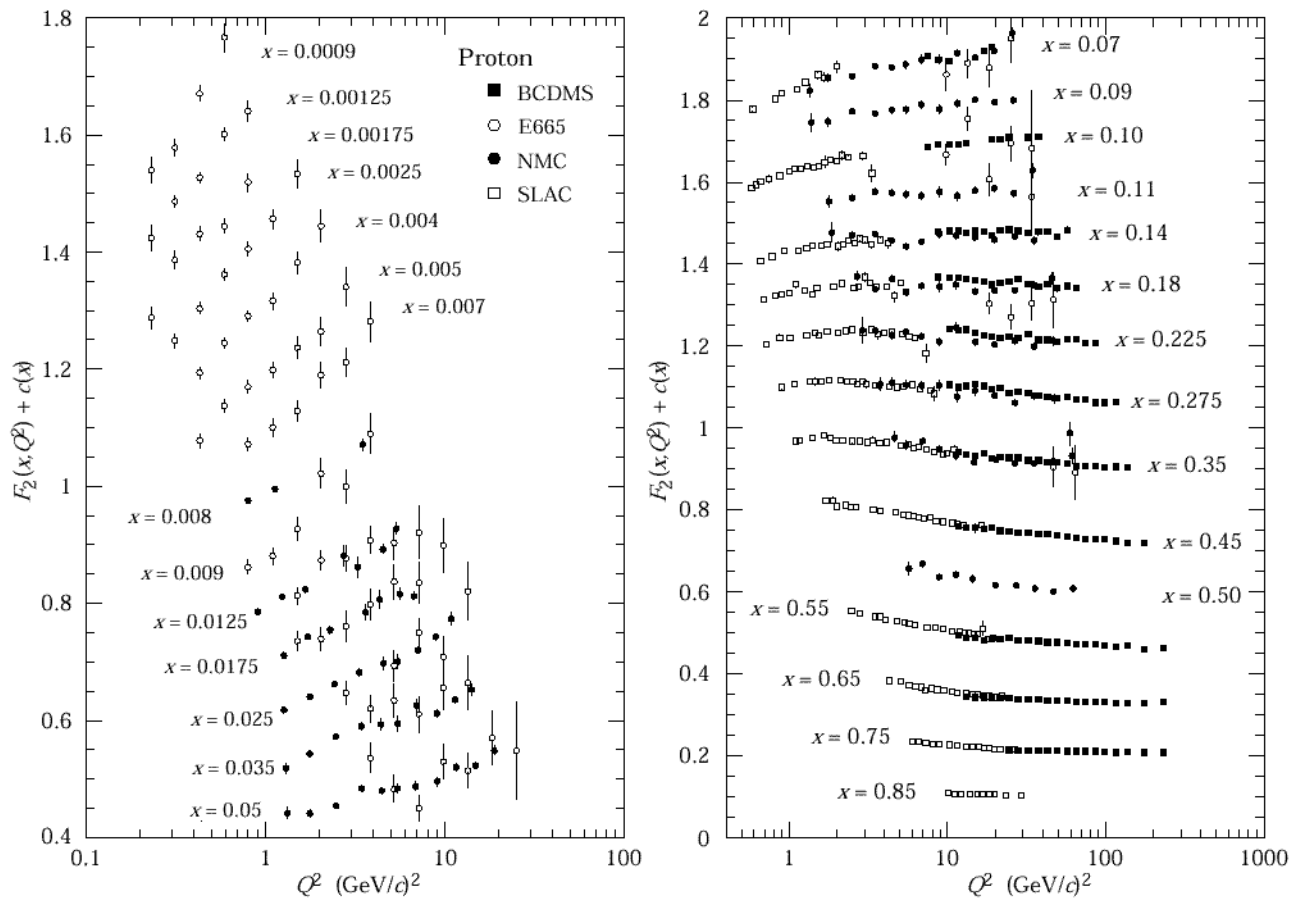


Figure 78: Structure functions  $F_2$  of proton from different experiments

- ❖ SLAC data from 1969 were first evidence of *partons*



Figure 79: SLAC's End Station A: proton target (left) and spectrometers

- ❖ The observed approximate scaling behaviour can be explained if protons are considered as composite objects
  - 🎯 *Scaling violation* is observed at very small and very big  $x$ : evidence of higher-order effects

- ❖ The trivial *parton model* assumes that proton consists of some partons; interactions between partons are not taken into account.
- ❖ Measured cross-section at any given  $x$  is proportional to the probability of finding a parton with a fraction  $z=x$  of the proton momentum

If there are several partons,

$$F_2(x, Q^2) = \sum_a e_a^2 x f_a(x) \quad (130)$$

where  $f_a(x)dx$  is the probability of finding parton  $a$  with fractional momentum between  $x$  and  $x+dx$ .

- ❖ Parton distributions  $f_a(x)$  are not known theoretically  $\Rightarrow F_2(x)$  has to be measured experimentally
  - ☉ However,  $f_a(x)$  are predicted to be the same for all  $Q^2$

While form (130) does not depend on the spin of a parton, predictions for  $F_1$  do:

$$F_1(x, Q^2) = 0 \quad (\text{spin-0})$$

$$2xF_1(x, Q^2) = F_2(x, Q^2) \quad (\text{spin-1/2}) \quad (131)$$

- ❖ The expression for spin-1/2 is called *Callan-Gross relation* and is very well confirmed by experiments  $\Rightarrow$  most evidently partons are quarks (!)
- ❖ Comparing proton and neutron structure functions and those from neutrino scattering, squared charge  $e_a^2$  of Eq.(130) can be evaluated; it appears to be consistent with square charges of quarks.